DEM-Aided Bundle Adjustment With Multisource Satellite Imagery: ZY-3 and GF-1 in Large Areas

Maoteng Zheng and Yongjun Zhang

***Abstract*—In this letter, a new digital elevation model (DEM)-aided bundle block adjustment (BBA) method is proposed which utilizes a rational-polynomial-coefficient affine transformation model and a preconditioned conjugate gradient (PCG) algorithm with multisource satellite imagery (ZY-3 and GF-1) for producing and updating ortho maps of large areas. To deal with the weak geometry of the large blocks, a reference DEM is used in this method as an additional constraint in the BBA. The PCG algorithm is applied to solve the large normal matrix produced by the massive data of the large areas. Our proposed method was tested on three blocks of real data collected by GF-1 panchromatic and multispectral sensors and ZY-3 three-line-camera sensors. The preliminary results show that the proposed method can achieve an accuracy of better than 0.5 pixels in planimetry and is suitable for wide application in ortho-map production. It also has great potential for the ortho-map production of superlarge areas such as the country of China as one block.**

***Index Terms*—Digital elevation model (DEM)-aided bundle block adjustment (BBA), multisource imagery, ortho-map production, preconditioned conjugate gradient (PCG), weak convergence geometry.**

I. Introduction

INCREASINGLY more high-resolution remote sensing satellites have been launched in China in recent years. The most well-known satellites are the first commercial stereo mapping satellite ZY-3 [1] and the high-resolution satellites GaoFeng (GF) series (including GF-1/2 and the recently launched GF-4, which is a geostationary orbit satellite). The ZY-3 satellite is integrated with a three-line camera (TLC) sensor to acquire stereo image pairs, which consists of three cameras pointing forward, nadir, and backward, respectively. The ground sampling distance (GSD) of the nadir camera is about 2.1 m, while the GSDs of the forward and backward cameras are about 3.2 m [1]. The GF-1 is integrated with two panchromatic and multispectral (PMS) sensors, both of which having a GSD of 2 m for panchromatic images [2]. Hundreds of thousands of images are collected and transmitted to the ground station from the ZY-3 and GF series satellites every day. A large portion of this imagery is available for the ortho-map production of large areas, such as a whole province or even the entire country of China.

Satellite images are generally released in scenes and rational polynomial coefficients (RPCs), as are the ZY-3 and GF-1 images. To cover a large block with the least number of images possible, the overlap areas between scenes are relatively small. The planimetry accuracy was the main concern for the proposed method since our purpose is to update and produce the ortho map. The base-to-height ratio of the overlap area in the flight direction (along track) is small due to the linear push-broom imaging system, and the overlap area between the images perpendicular to the flight direction (across track) has weak geometry structures. This situation is not desirable since it may cause erroneous results or iteration failures during the bundle block adjustment (BBA). Thus, we used a reference digital elevation model (DEM) as an additional constraint in the BBA.

Large areas contain more data, which then consequently produce large normal equations in BBA. If the normal matrix was not structured, the traditional BBA method was no longer appropriate for our very large normal equations due to its memory limitation. For example, if the country of China was set as one block, the image number was estimated to be no less than 5000. The rational functional model's (RFM's) affine transformation model is applied to conduct BBA, and the data type is double; then, the memory requirement of the normal matrix will be $5000 * 6 * 5000 * 6 * 8$ B ≈ 6.7 GB. This is a very large memory requirement for a common computer. Even if computers have enough memory space for this large matrix, the computation speed likely will be very low since a sizable part of their RAM is occupied as well. If the unknown parameters can be properly ordered to obtain a structured normal matrix, the classical Cholesky factorization method for a sparse normal matrix can be applied. However, we choose a new algorithm: the preconditioned conjugate gradient (PCG) algorithm instead to determine the normal equation in this letter.

The main objective of the research presented in this letter is to develop a method for ortho-map production and updating in large areas, such as specific provinces or even the entire country of China, with a reference DEM using multisource satellite imagery (ZY-3 and GF-1). To deal with the weak geometry of the large blocks, a modified DEM-aided BBA with an RFM affine transformation model is created. The PCG algorithm is utilized to solve the large normal matrix produced by the massive acquired data of large areas in the BBA. Three blocks of real data collected by a GF-1 PMS sensor and a ZY-3 TLC

Manuscript received February 7, 2016; revised March 28, 2016 and April 2, 2016; accepted April 5, 2016. Date of publication April 27, 2016; date of current version May 19, 2016. This work was supported in part by the National Natural Science Foundation of China under Grant 41322010, by the China Postdoctoral Science Foundation under Grant 2015M572224, by the Key Laboratory for Aerial Remote Sensing Technology of the National Administration of Surveying, Mapping and Geoinformation under Grant 2014B01, and by the Fundamental Research Funds for the Central Universities, China University of Geosciences (Wuhan) under Award CUG160838.

M. Zheng is with the National Engineering Research Center for Geographic Information System, China University of Geosciences, Wuhan 430074, China (e-mail: tengve@163.com).

Y. Zhang is with the School of Remote Sensing and Information Engineering, Wuhan University, Wuhan 430079, China (e-mail: zhangyj@whu.edu.cn).

Color versions of one or more of the figures in this paper are available online at http://ieeexplore.ieee.org.

Digital Object Identifier 10.1109/LGRS.2016.2551739

nadir camera were tested with our proposed method. As the application of ortho mapping in large areas continues to rapidly increase, this method can greatly enable the wide and full use of the ever-increasing number of remote sensing images. It also has potentials for ortho-map production in superlarge areas such as the entire country of China.

The remainder of this letter is organized in four sections. Related studies, methods, and techniques in the literature are reviewed in Section II. The methodology of the DEM-aided BBA, RFM affine transformation model, and PCG algorithm are introduced and discussed in Section III. Our applications with real data and the analysis of the results are presented in Section IV. Finally, the overall conclusions are given in Section V.

II. Related Works

Many researchers have studied the geometric and radiometric characteristics of satellite images. Zhang *et al.* calibrated the TLC sensor of ZY-3 with multiorbit data and improved its direct orientation accuracy from 1 km to better than 20 m in both plane and height [1]. GF-1 is the first civil high-resolution satellite in China. Several past studies and applications with GF-1 imagery focused on its radiometric perspective [3]–[5]. However, only a few researchers addressed GF-1's geometric performance even though it is also an important topic.

RPCs and the rational functional model (RFM) [6], well known and widely used in the distribution and processing of satellite imagery, have been proven to be very simple, fast, and stable. DEM-aided BBA with RPCs has been studied and implemented by others [8], [9], [17], but the authors again used only a few images in a small area for their experiments except Angelo and Reinartz who implemented BBA with 810 scenes of Catosat-1 imagery [17]. However, they applied the traditional BBA method and stored the normal matrix which could be suffered by the memory requirement when dealing with more images; moreover, they used a digital surface model to decrease the requirement of ground point coordinate (GCP) number not to compensate the poor convergence as discussed in this letter. Zhang *et al.* conducted experiments in large areas using the multiorbits of TLC imagery with no GCPs, but because the authors performed BBA using a strict physical model with long-orbit data rather than small scene images with RPC, the unknown number was relatively small [7]. The BBA based on RPC for large areas is not considered practical due to the memory limitation for the normal equation of the traditional BBA method on a common computer.

The conjugate gradient (CG) algorithm was introduced for the first time in 1952 [10], but it is not widely used due to its drawbacks in precision and stability until recently. This method multiplies the normal matrix to the residual vector of the normal equation, forming a Krylov subspace [11]; then, it iteratively computes the answer of the normal equation and eventually reaches a convergence value that is close enough to the true answer [10]. The CG algorithm was extended to an advanced method called PCG, which uses a preconditioner to reduce the condition of the normal matrix so as to improve the converging speed [12]–[16].

III. Methodology

A. RFM Affine Transformation Model

RFM uses a rational polynomial to express the relationship between the image coordinates and the corresponding ground coordinates as shown in (1). The coefficients are the so-called RPCs

$$\begin{cases} x = \frac{Num_x(X,Y,Z)}{Den_x(X,Y,Z)} \\ y = \frac{Num_y(X,Y,Z)}{Den_y(X,Y,Z)} \end{cases} \tag{1}$$

where $Num_x(X,\ Y,\ Z)$, $Den_x(X,\ Y,\ Z)$, $Num_y(X,\ Y,\ Z)$, $Den_y(X,Y,Z)$ are third-order rational polynomials about (X,Y,Z), each of which has 20 coefficients.

A total of 80 coefficients plus 10 normalization parameters make up a group of RPCs that can be used to transfer the GCPs to the corresponding image point coordinates. This model is widely applied in the processing of satellite imagery, particularly in ortho-map production. To correct and refine RPC, the most common and stable method is the affine transformation model as shown in

$$\begin{cases} x = a_0 + a_1 x' + a_2 y' \\ y = b_0 + b_1 x' + b_2 y' \end{cases} \tag{2}$$

where x', y' are the calculated image point coordinates by RPC and x, y are the observations of the image point coordinates. $a_0, a_1, a_2, b_0, b_1, b_2$ are the affine transformation parameters.

The error equation can be established as follows:

$$\mathbf{V} = [\mathbf{A} \quad \mathbf{B}] \begin{bmatrix} \mathbf{s} \\ \mathbf{t} \end{bmatrix} - \mathbf{l} \tag{3}$$

where $\mathbf{V}$ is the residual vector, $\mathbf{A}$ is the design matrix which consists of partial derivatives of x, y to $a_0, a_1, a_2, b_0, b_1, b_2$, respectively, $\mathbf{B}$ is the design matrix which consists of partial derivatives of x, y to X, Y, Z, respectively, $\mathbf{s}$ is the correction vector of affine parameters, $\mathbf{t}$ is the correction vector of the unknown GCPs, and $\mathbf{l}$ is the difference of the calculated and observed image point coordinates.

Applying the Gauss–Newton model, we can obtain the normal equation as follows:

$$\begin{bmatrix} \mathbf{A^T PA} & \mathbf{A^T PB} \\ \mathbf{B^T PA} & \mathbf{B^T PB} \end{bmatrix} \begin{bmatrix} \mathbf{s} \\ \mathbf{t} \end{bmatrix} = \begin{bmatrix} \mathbf{A^T Pl} \\ \mathbf{B^T Pl} \end{bmatrix} \tag{4}$$

where $\mathbf{P}$ is the weight matrix.

For simplicity, we can rewrite (4) as

$$\begin{bmatrix} \mathbf{U} & \mathbf{W} \\ \mathbf{W}^{\boldsymbol{T}} & \mathbf{V} \end{bmatrix} \begin{bmatrix} \mathbf{s} \\ \mathbf{t} \end{bmatrix} = \begin{bmatrix} \mathbf{l}_{\boldsymbol{u}} \\ \mathbf{l}_{\boldsymbol{v}} \end{bmatrix}. \tag{5}$$

As can be seen in (4), matrices $\mathbf{U}$ and $\mathbf{V}$ are both block diagonal, and the number of ground point unknowns $\mathbf{t}$ is always much more than that of the image-related unknowns $\mathbf{s}$. Therefore, we can eliminate the ground point unknowns using a blockwise Gauss elimination method and obtain the reduced normal equation (6)

$$(\mathbf{U} - \mathbf{W}\mathbf{V}^{-1}\mathbf{W}^{\boldsymbol{T}})\mathbf{s} = \mathbf{l}_{\boldsymbol{u}} - \mathbf{W}\mathbf{V}^{-1}\boldsymbol{l}_{\boldsymbol{v}} \tag{6}$$

$$\mathbf{V}\mathbf{t} = \mathbf{l}_{\boldsymbol{v}} - \mathbf{W}^{\boldsymbol{T}}\boldsymbol{s}. \tag{7}$$

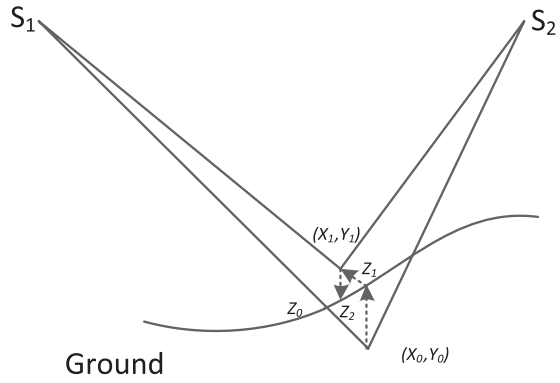

Fig. 1. DEM-aided intersection for GCPs.

Unknown parameters $\mathbf{s}$ can be calculated by (6), and $\mathbf{t}$ can then be substituted by (7). In this letter, the ground point unknowns $\mathbf{t}$ are intersected by image-related unknowns $\mathbf{s}$ and RPCs with DEM as the control data as shown in Fig. 1. If there are m images and n points, the size of the normal matrix now is reduced from $(6\ m + 3\ n) * (6\ m + 3\ n)$ to $6\ m * 6\ m$. This process is the so-called Schur complement trick. Matrix $\mathbf{U} - \mathbf{W}\mathbf{V}^{-1}\mathbf{W}^{T}$ is known as the Schur complement matrix. Note that $m \gg n$ is the usual case; thus, the Schur complement can reduce the size of the normal matrix efficiently.

B. DEM-Aided Intersection for Ground Points

To deal with the weak convergence geometry and small base-to-height ratio situation, a reference DEM is used in the intersection for the ground points. First, an initial altitude Z_0 is given, and the corresponding planimetry coordinates X_0, Y_0 are calculated by RPC and affine transformation parameters. Then, we interpolate a new altitude Z_1 from DEM with X_0, Y_0, after a few iterations, when the incremental value of the new altitude $(Z_{i+1}\text{-}Z_i)$ is smaller than a certain threshold; then, the iteration is over. The full procedure is demonstrated in Fig. 1.

C. PCGs

The PCG algorithm is an advanced algorithm that originated from the CG algorithm (details of CG can be found in [10]).

The PCG method multiplies preconditioner $\mathbf{M}^{-1}$ to the normal matrix so as to decrease the condition of the normal matrix and thus accelerate the iteration process. After using a preconditioner, linear equation (8)

$$\mathbf{B}\mathbf{x} = \mathbf{c} \tag{8}$$

can be rewritten as

$$\mathbf{M}^{-1}\mathbf{B}\mathbf{x} = \mathbf{M}^{-1}\mathbf{c}. \tag{9}$$

The number of iterations should be no more than the condition of matrix $\mathbf{M}^{-1}\mathbf{B}$. The main task is now shifted to finding a proper precondition matrix which can decrease the condition of the normal matrix and is easy to be inverted. The simplest and most widely used preconditioner is the block Jacobi preconditioner which is the block diagonal of the normal matrix. Other preconditioners, including the symmetric-successive-overrelaxation preconditioner [12], the QR factorization preconditioner [13], the balanced incomplete factorization-based preconditioner [14], the multiscale preconditioner [15], and the subgraph preconditioner [16], could be more efficient but might be more complicated and less stable. In this letter, we apply the block Jacobi preconditioner.

TABLE I
STATISTICAL INFORMATION OF TEST DATA

Block	Location	Area (km^2)	Image number	TP number	GCP number
1	Anhui	140,000	154	85586	30262
2	Henan	167,000	176	98163	33074
3	Jiangxi	166,900	183	105650	0

D. Accuracy Analysis

Only planimetry accuracy is assessed in this letter since our application goal is to update an ortho map and also because the DEM is used as the control data in the BBA. In order to fully assess the accuracy of our proposed method, two accuracy terms, absolute/external accuracy and relative/internal accuracy, are investigated. The absolute accuracy is verified by checkpoints (CKPs) as in the traditional BBA procedure.

Good relative accuracy ensures good performance in the image mosaic process. Relative accuracy is verified by image point residuals known as reprojection error. The image point residuals can be calculated by the following equation:

$$\begin{aligned} r_x &= a_0 + a_1 x_{rpc} + a_2 y_{rpc} - x \\ r_y &= b_0 + b_1 x_{rpc} + b_2 y_{rpc} - y \end{aligned} \tag{10}$$

where r_x, r_y are the residuals of image point coordinates, x_{rpc}, y_{rpc} are the image point coordinates determined by RFM, x, y are the image point observations, and $a_0, a_1, a_2, b_0, b_1, b_2$ are the affine transformation parameters.

IV. EXPERIMENTS AND ANALYSIS

A. Data Set

The real data were collected by the nadir camera of the ZY-3 TLC sensor and the GF-1 PMS sensor. All the images were provided with their corresponding RPC data. A total of three blocks of imagery were tested. The detail information of the data set is listed in Table I. The tie points (TPs) were extracted by our research team, and the details of the image matching are omitted here since we focused on only BBA methods and techniques in this letter. The GCPs were also automatically extracted using the old ortho map as the reference. They are distributed in every scene of block 1 and block 2 despite that fact that the GCP number of each scene is different. The ground footprints of these blocks are shown in Fig. 2.

The reference old DEM for BBA and the reference old ortho map for the automatic extraction of GCPs were both provided by the National Administrator of Surveying, Mapping, and Geoinformation. The accuracy of the DEM is about 10 m in height, and the planimetry accuracy of the ortho map is about 2–3 m.

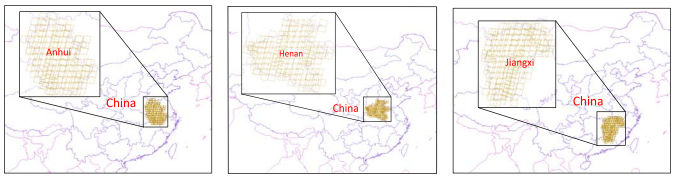

(a) (b) (c)

Fig. 2. Ground coverage of the three blocks. The larger black rectangle is an enlarged version of the smaller black rectangle.

TABLE II
COMPARISON RESULTS OF BBA WITH THREE BLOCKS

Blocks	Images	Initial accuracy				DEM-aided adjustment					
		Absolute Error (m)		Relative Error (pixel)		GCP Residuals (m)		CKP Absolute Error (m)		Relative Error(pixel)	
		X	Y	x	y	X	Y	X	Y	x	y
Anhui	154	23.0	20.8	12.2	10.1	1.84	1.69	1.76	1.72	0.37	0.39
Henan	176	26.6	28.5	16.4	23.5	1.72	1.93	1.74	1.94	0.41	0.49
Anhui (no GCP)	154	23.1	20.8	12.2	10.1	N/A	N/A	2.6	4.4	0.55	1.20
Henan (no GCP)	176	26.6	28.5	16.4	23.5	N/A	N/A	2.3	4.1	0.43	0.89
Jiangxi	183	N/A	N/A	5.1	8.37	N/A	N/A	N/A	N/A	0.52	1.75

B. Weight Strategy

An effective and stable weight strategy was applied to eliminate the gross points. The initial weights of the image point observations were set as the unit weights, which were recalculated during each iteration using the residuals of the image point coordinates computed according to (10). If the residuals were larger than the threshold value, meaning that the current image point was a blunder, then the weights of the corresponding image point observations were set as a much smaller value as shown in (12)

$$p_0 = 1 \tag{11}$$

$$p_{i+1} = \begin{cases} p_i & r < c \\ p_i * s & r \geq c \end{cases} \tag{12}$$

where p_i is the weight of the ith iteration and s is a coefficient between (0, 1) aiming to decrease the weight of gross points. r is the residual of the image point, and c is the threshold value of the residual.

C. DEM-Aided BBA With the Three Large Blocks

The initial accuracies of direct orientation with the provided RPCs were first examined by all the GCPs. Then, we conducted the DEM-aided BBA with all three blocks. Half of the GCPs were used as CKPs, and the other half were used as control points. The comparison results, including the initial accuracy and the accuracy with or without GCP after adjustments, are listed in Table II, except the absolute accuracy which could not be verified in block 3 since no GCP was provided. The detailed distributions of the part of the image point residuals before and after BBA are demonstrated in Fig. 3.

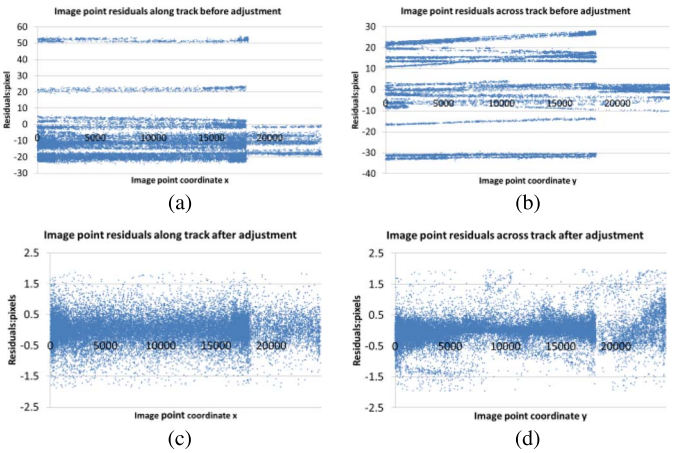

(a) (b) (c) (d)

Fig. 3. Part of the image point distribution before and after BBA. To explicitly show the details, the scales of vertical axes in these figures are different before and after BBA. (a) and (b) show the image point residuals along track and across track before adjustment, and (c) and (d) show the image point residuals along track and across track after adjustment.

As shown in Table II, the initial absolute accuracies are worse than 20 m, and the relative accuracies are worse than 10 pixels. After BBA with DEM and GCP, both the absolute and relative accuracies are improved greatly to about 1.7 m and 0.5 pixels. When there is no GCP involved, the relative errors are worse than that with GCPs, particularly in the y-direction (across track) where the error is up to 1.75 pixels, which is not a desirable accuracy. This result could be due to the weak convergence geometry and the absence of GCPs. We suggest that the weak convergence condition should be compensated by both the DEM data and a number of GCPs (not sparse GCP) in order to achieve considerable accuracy. For the two blocks with GCPs, the distributions of their image point residuals are shown in Fig. 3. Some of the initial image point residuals are quite large (up to 60 pixels) before BBA and are different for different images as shown in Fig. 3(a) and (b). After the BBA procedure, the image point residuals are greatly decreased and distributed evenly between $(-2, 2)$ pixels as shown in Fig. 3(c) and (d). The accuracy of less than 0.5 pixels is preferable in the mosaic of ortho maps, which indicates that our proposed method is effective and reasonable.

D. Potential for Nationwide BBA

In this letter, the proposed method is successfully applied to three provinces of China. Our future goal is to directly perform DEM-aided BBA for the country of China or even the whole world. There is one main bottleneck for this undertaking: the big data issue. As mentioned earlier, a block covering the entire country of China will need more than 5000 scenes of images (ZY-3 and GF-1 imagery). The normal matrix in the BBA could be superlarge, and the storage and inversion of this large matrix is a difficult problem in the traditional BBA method. Since our method applies the PCG algorithm to solve the normal equation, it does not explicitly store and invert the normal matrix, thereby eliminating the big data as an issue in our method. Once the test data are available, we could perform DEM-aided BBA to the country of China.

TABLE III
ESTIMATED MEMORY REQUIREMENTS OF BBA WITH THE TRADITIONAL METHOD AND THE PROPOSED METHOD FOR LARGE AREAS

Image number	Memory requirement of traditional method (GB)			Memory requirement of proposed method (GB)		
	Image points & RPC data	Normal matrix	Total	Image points & RPC data	Normal matrix	Total
5000(Entire China)	0.5	6.7	7.2	0.5	0.0	0.5
10000	1.0	26.8	27.8	1.0	0.0	1.0
100000	10 .0	2680 .0	2690.0	10.0	0.0	10.0

To estimate the size of the data for the country of China as a block, we assume that the image density was the same for the aforementioned three provinces. For example, the raw data (including the image points and RPC data) is about 16 MB in the Anhui block, which consists of 154 images, so the size of the raw data for one China block should be $16 * 5000/154 = 0.5$ GB since the data size increases linearly with respect to the image number. However, the size of the normal matrix increases exponentially as the image number is increasing; the memory requirement of the normal matrix should be 6.7 GB as mentioned earlier. The memory requirements of the BBA traditional method and our proposed method in some superlarge blocks are listed in Table III.

As can be seen in Table III, the memory requirement for the normal matrix increases exponentially with respect to the image number. The normal matrix therefore is too large for storage in the traditional method for the blocks with more than 5000 images in a common computer. Despite some computers having enough memory to accommodate these images, their computation ability would be compromised because most of the RAM also would be occupied. However, the proposed method does not need to store the normal matrix, rather only the image points, RPC data, and a few vectors. The total memory requirement of a block with 5000 images is only 0.5 GB, which is available nowadays in most computers. When the image number is increased to 10 000, the memory requirement is about 27.8 GB which can be hardly spared even for a workstation with 32-GB RAM. We believe our method therefore is capable of performing BBA for the country of China as one block; furthermore, it has potential for application to larger blocks of tens of thousands, and even hundreds of thousands, of images.

V. CONCLUSION

A new DEM-aided BBA method with weak convergence geometry for large areas is proposed in this letter. The RPC affine transformation model in the proposed method is applied to conduct BBA, and a PCG algorithm is introduced to deal with the large normal matrix produced by the big data of superlarge blocks. The current test data involve only a few provinces of China, but we intend to conduct BBA with the country of China as one block in the future. The weak convergence geometry caused by the small overlap, both along and across track, and the small base-to-height ratio along track could lead to the unstable solution in the BBA. Thus, a reference DEM is utilized for the control data. After the full analysis of the experiment results, we conclude the following.

1) The proposed method improves the accuracy of ZY-3 and GF-1 imagery greatly, from worse than 20 pixels to better than 0.5 pixels, despite the relative low accuracy in the y-direction (across track) in block 3 due to the absence of GCP.
2) The weak convergence geometry in the block is strengthened by the reference DEM in the BBA.
3) Our model is capable of producing ortho maps of large areas, such as the three provinces of China used for data in this letter. The ortho-map production of an even larger area as a block, such as the country of China, is now a strong possibility with our precise and practical method.

REFERENCES

[1] Y. J. Zhang, M. T. Zheng, J. X. Xiong, Y. H. Lu, and X. D. Xiong, "On-orbit geometric calibration of ZY-3 three-line array imagery with multistrip data sets," *IEEE Trans. Geosci. Remote Sens.*, vol. 52, no. 1, pp. 224–234, Jan. 2014.
[2] S. C. Huang, H. P. Wu, and D. C. Feng, "Ortho accuracy analysis of GF-1 PAN imagery," *Remote Sens. Inf.*, vol. 30, no. 2, pp. 85–88, 2015.
[3] A. X. Yang, B. Zhong, W. B. Lv, S. L. Wu, and Q. H. Liu, "Cross-calibration of GF-1/WFV over a desert site using Landsat-8/OLI imagery and ZY-3/TLC data," *Remote Sens.*, vol. 7, no. 8, pp. 10 763–10 787, Aug. 2015.
[4] L. Feng *et al.*, "Radiometric cross-calibration of Gaofen-1 WFV cameras using Landsat-8 OLI images: A solution for large view angle associated problems," *Remote Sens. Environ.*, vol. 174, pp. 56–68, Mar. 2016.
[5] J. Li, X. L. Chen, L. Q. Tian, J. Huang, and L. Feng, "Improved capabilities of the Chinese high-resolution remote sensing satellite GF-1 for monitoring suspended particulate matter (SPM) in inland waters: Radiometric and spatial considerations," *ISPRS J. Photogramm. Remote Sens.*, vol. 106, 145–156, Aug. 2015.
[6] J. Grodecki and G. Dial, "Block adjustment of high-resolution satellite images described by rational functions," *Photogramm. Eng. Remote Sens.*, vol. 69, no. 1, pp. 59–70, Jan. 2003.
[7] Y. J. Zhang, M. T. Zheng, X. D. Xiong, and J. X. Xiong, "Multi-strips bundle block adjustment of ZY-3 satellite imagery by rigorous sensor model without ground control points," *IEEE Geosci. Remote Sens. Lett.*, vol. 12, no. 4, pp. 865–869, Apr. 2015.
[8] T. A. Teo, L. C. Chen, C. L. Liu, Y. C. Tung, and W. Y. Wu, "DEM-aided block adjustment for satellite images with weak convergence geometry," *IEEE Trans. Geosci. Remote Sens.*, vol. 48, no. 4, pp. 1907–1918, Apr. 2010.
[9] T. Toutin, "Geometric processing of Ikonos geo images with DEM," in *Proc. Joint ISPRS Workshop High Resol. Mapping Space*, Sep. 19–21 2001, Hannover, Germany, p. 9.
[10] M. R. Hestenes and E. Stiefel, "Methods of conjugate gradients for solving linear system," *J. Res. Nat. Bureau Std.*, vol. 49, no. 6, pp. 409–436, 1952.
[11] Y. Saad, "Krylov subspace methods for solving large unsymmetric linear systems," *Math. Comput.*, vol. 37, no. 155, pp. 105–126, 1981.
[12] S. Agarwal *et al.*, "Bundle adjustment in the large," in *Computer Vision—ECCV*. Berlin, Germany: Springer-Verlag, 2010, pp. 29–42.
[13] M. Byröd and K. Åström, "Conjugate gradient bundle adjustment," in *Computer Vision—ECCV*, vol. 6312, ser. Lecture Notes in Computer Science. Berlin, Germany: Springer-Verlag, 2010, pp. 114–127.
[14] R. Bru, J. MarÍn, J. Mas, and M. Tůma, "Balanced incomplete factorization," *SIAM J. Sci. Comput.*, vol. 30, no. 5, pp. 2302–2318, 2008.
[15] M. Byröd and K. Åström, "Bundle adjustment using conjugate gradients with multiscale preconditioning," in *Proc. Brit. Mach. Vis. Conf.*, 2009, pp. 1–10.
[16] Y. D. Jian, D. C. Balcan, and F. Dellaert, "Generalized subgraph preconditioners for large-scale bundle adjustment," in *Proc. IEEE Int. Conf. Comput. Vis.*, 2011, vol. 6669, pp. 295–302.
[17] P. D. Angelo and P. Reinartz, "DSM based orientation of large stereo satellite image blocks," *Int. Arch. Photogramm., Remote Sens. Spatial Inf. Sci.*, vol. 39, no. B1, pp. 209–214, 2012.